

Dioxane and oxathiane nuclei: Suitable substructures for muscarinic agonists

Alessandro Piergentili,^{a,*} Wilma Quaglia,^a Mario Giannella,^a Fabio Del Bello,^a Bruno Bruni,^b Michela Buccioni,^a Antonio Carrieri^c and Samuele Ciattini^d

^aDipartimento di Scienze Chimiche, Università degli Studi di Camerino, Via S. Agostino, 1, 62032 Camerino, Italy

^bDipartimento di Chimica, Università degli Studi di Firenze, Via della Lastruccia, 3, 50019 Sesto Fiorentino, Firenze, Italy

^cDipartimento Farmaco-Chimico, Università degli Studi di Bari, Via E. Orabona, 4, 70125 Bari, Italy

^dCentro Interdipartimentale di Cristallografia, Università degli Studi di Firenze, Via della Lastruccia, 3, 50019 Sesto Fiorentino, Firenze, Italy

Received 31 August 2006; revised 16 October 2006; accepted 19 October 2006

Available online 21 October 2006

Abstract—Muscarinic agonists, bearing 1,4-dioxane and 1,4-oxathiane nuclei, were synthesized and tested to evaluate their potency at M₁–M₄ muscarinic receptor subtypes. The stereochemical relationship between the 2-side chain and the 6-methyl group plays an important role in drug–receptor interaction, since the *cis* isomers are more potent than the corresponding *trans* isomers. However, the latter are able to discriminate between the muscarinic receptor subtypes. Among them compound **5b** proves particularly interesting, since it selectively activates the ileal M₃ receptor subtype and is devoid of agonist activity at the others.

© 2006 Elsevier Ltd. All rights reserved.

1. Introduction

The study of muscarinic agonists has been arousing great interest in recent years due to the numerous therapeutic properties mediated by the activation of the corresponding receptors.¹ On the basis of genetic and pharmacological characterizations, these receptors, belonging to the G-protein-coupled receptors (GPCRs) superfamily,² are subdivided into five different subtypes (M₁–M₅).³

Due to the different transduction mechanism, these five subtypes have been grouped into two series: the stimulation of those designated by odd numbers (M₁, M₃, and M₅) causes, above all, the activation of phospholipase C, leading to the formation of phosphatidyl-inositol (IP₃) and diacylglycerol (DAG) and intracellular Ca²⁺ mobilization, whereas the stimulation of those designated by even numbers (M₂ and M₄) produces adenylyl cyclase inhibition and the consequent reduction of AMPc

levels.⁴ Recent studies suggest that M₂, M₃, and M₄ subtypes are expressed in staminal cells, whose proliferation and neurogenesis are modulated by the endogenous ligand acetylcholine (ACh).⁵ Besides, the ability of ACh to stimulate the DNA synthesis of neuronal cells had already been described 15 years ago in primary astrocytes.⁶ In the CNS, the muscarinic receptors are involved in motor control, cardiovascular and corporeal temperature regulation, and memory. In the periphery, they mediate smooth muscle contraction, glandular secretion, and regulation of cardiac rate and force.⁴ Therefore, the potential therapeutic applications of ligands interacting with such receptors are numerous, though the clinical use is limited by various side effects due to the lack of a marked subtype-discrimination. The low selectivity, which is rarely more than 100-fold higher for one subtype with respect to the others, seems to be due to the high aminoacidic sequence homology of the five receptor subtypes.^{7,8}

The main applications of the muscarinic agonists concern the treatment of cognitive disorders in Alzheimer's disease (AD), in which M₁ selective agonists are able to improve learning and memory.⁹ Moreover, the activation of this receptor subtype causes a significant reduction of β -amyloid peptide (A β) release via the stimulation of phosphatidyl-inositol hydrolysis.¹⁰

Keywords: Muscarinic agonists; Subtype selectivity; 1,4-Dioxane nucleus; 1,4-Oxathiane nucleus.

* Corresponding author. Tel.: +39 0737 402237; fax: +39 0737 637345; e-mail: alessandro.piergentili@unicam.it

The beneficial effects in AD psychotic behaviors suggest the use of muscarinic agonists in the treatment of schizophrenia, in which dopamine release may be reduced by the stimulation of M_1 and M_4 heteroreceptors or by the inhibition of M_2 autoreceptors, which, in their turn, modulate ACh release.¹¹ The observation that muscarinic analgesia is mediated by a combination of M_2 and M_4 subtypes at spinal and supraspinal levels makes the corresponding ligands, endowed with agonist activity, promising anti-nociceptive agents.^{12,13} Moreover, the activation of muscarinic receptors has been shown to be neuroprotective in several different models of apoptosis;¹⁴ the exact action mechanism is not yet known, but it has been demonstrated that the M_3 muscarinic receptor anti-apoptotic response is independent of calcium/phospholipase C signaling.¹⁵

Most muscarinic agonists possess a conformationally constrained structure with respect to the endogenous ligand ACh¹⁶ and, among them, one of the most potent is the *cis*-trimethyl-(2-methyl-[1,3]dioxolan-4-ylmethyl)-ammonium iodide (**1a**); this was prepared together with its corresponding *trans* isomer (**1b**) over 40 years ago¹⁷ and, at that time, defined a ‘supermuscarinic agent’. Subsequently, it was demonstrated that its *cis*-1,3-oxathiolane analogue (**2a**) showed similar muscarinic potency.^{18,19}

Some studies, among which one of ours,²⁰ have reported that ligands bearing a hexacyclic structure are endowed with cholinergic activity.^{21,22} Also the higher homologues of compound **1a**, *cis*-trimethyl-(2-methyl-[1,3]dioxan-4-ylmethyl)-ammonium iodide (**3a**),^{23,24} and its corresponding 1,4-dioxane regioisomer (**4** as a *cis/trans* mixture)²¹ have been reported to show a parasympathomimetic action. However, in these papers, accurate activity–stereochemistry relationships of the molecules and a complete pharmacological study at all the four muscarinic subtypes were not investigated. Therefore, in the present study, the higher homologues of **1** and **2** were synthesized, and the *cis* and *trans* isomers were separated (compounds **4a**, **4b** and **5a**, **5b**, respectively). Moreover, the *cis* form (\pm)-**4a** was resolved into the corresponding enantiomers. Finally, compounds **1a**, **1b**,

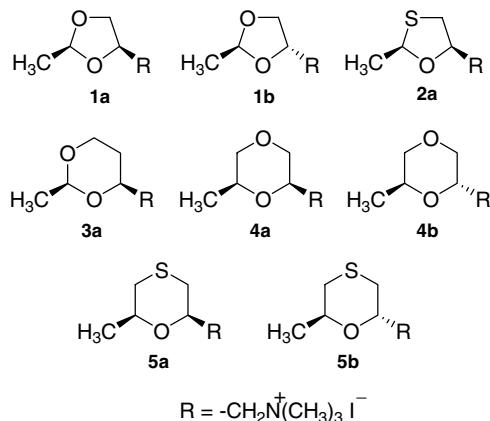


Figure 1.

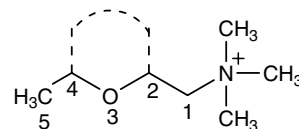


Figure 2.

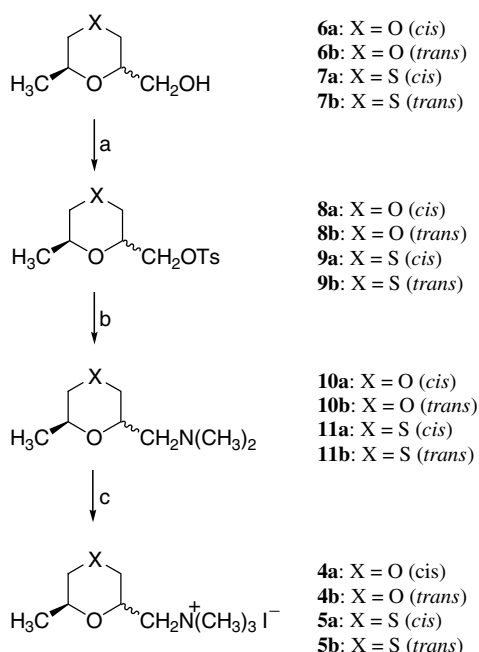
and **3a** were synthesized and included in the pharmacological study (Fig. 1).^{17,23,25}

All the compounds examined bear the archetypical structure of classical muscarinic agonists, such as ACh, muscarine, and 1,3-dioxolane **1a** (Fig. 2). However, though respecting Ing's rule of the ‘5-atom chain’,^{26,27} the different architecture of the backbone of the fourth N-substituent might determine different activities at the four muscarinic receptor subtypes and, consequently, a subtype-discrimination might be obtained.

2. Chemistry

The isomers **4a**, **4b** and **5a**, **5b** were obtained according to the reaction sequence reported in Scheme 1. The treatment of alcohols **6a**, **6b** and **7a**, **7b**^{28,29} with tosyl chloride and subsequent amination with dimethylamine afforded the corresponding amines **10a**, **10b** and **11a**, **11b**, which, treated with methyl iodide, gave compounds **4a**, **4b** and **5a**, **5b**, respectively.

The *cis* stereochemical relationship between the 2-side chain and the 6-methyl group of **4a**, assigned according to what has been reported in the literature for alcohols **6a**, **6b** and **7a**, **7b**,^{28,29} was confirmed through

Scheme 1. Reagents: (a) *p*-TsCl, pyridine; (b) $(CH_3)_2NH$, benzene; (c) CH_3I , diethyl ether.

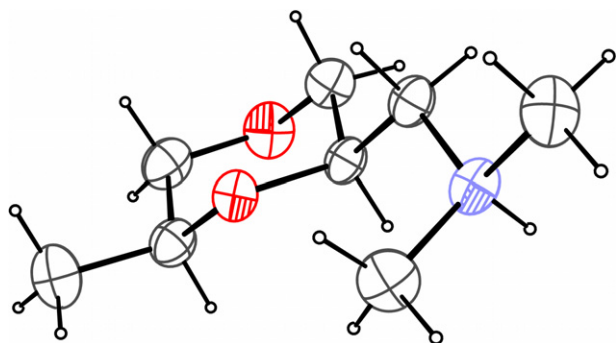


Figure 3. A view of the cation in the X-ray structure of the **10a** picrate salt; 30% probability ellipsoids are shown.

single-crystal X-ray diffraction analysis of the picrate salt of the corresponding base **10a** (Fig. 3).

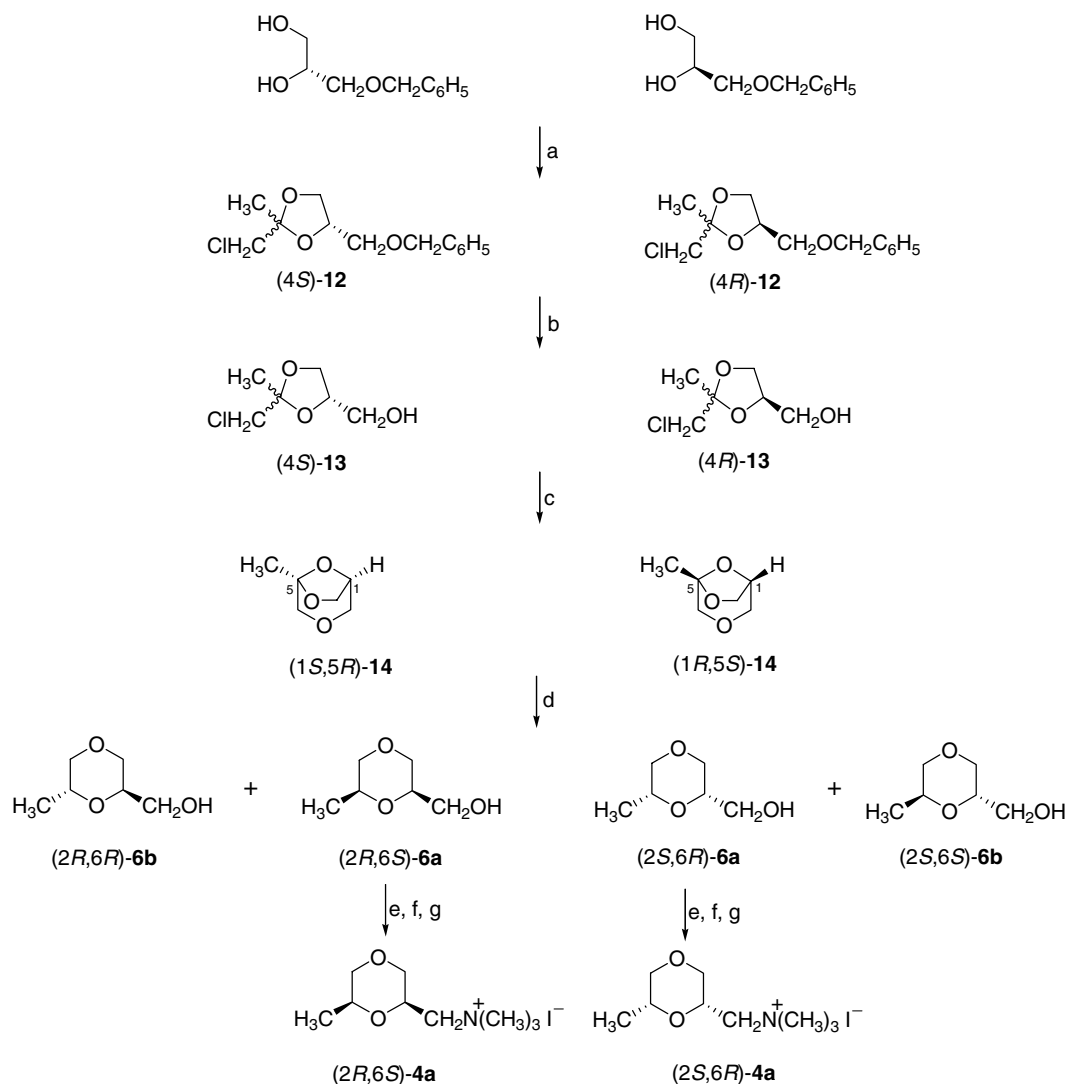
The two enantiomers of (\pm)-**4a** were prepared by stereoselective synthesis starting from (*R*)- or (*S*)-3-benzyloxypropane-1,2-diol, whose reaction with chloroacetone led to the corresponding diastereomeric forms (4*S*)- and (4*R*)-4-benzyloxymethyl-2-chloromethyl-2-methyl-[1,3]dioxolane [(4*S*)-**12** and (4*R*)-**12**; *cis/trans* ratio = 1:1] (Scheme 2). The hydrogenolysis with Pd(OH)₂ followed by the treatment with KOH and the subsequent regiospecific opening³⁰ of the bicyclo[3.2.1]octanes (1*S*,5*R*)-**14** and (1*R*,5*S*)-**14** afforded mixtures of the corresponding diastereomeric forms (2*R*,6*S*)-**6a**, (2*R*,6*R*)-**6b** and (2*S*,6*R*)-**6a**, (2*S*,6*S*)-**6b**, respectively. The diastereomers were separated by column chromatography. The *trans* enantiomeric forms (2*R*,6*R*)-**6b** and (2*S*,6*S*)-**6b** were obtained in poor yields and, therefore, it was not possible to proceed with the subsequent reaction and to obtain the corresponding final compounds. Finally, the two methiodides (2*R*,6*S*)-(+)-**4a** and (2*S*,6*R*)-(–)-**4a** were prepared by subjecting the enantiomeric alcohols (2*R*,6*S*)-(+)-**6a** and (2*S*,6*R*)-(–)-**6a** to the same reaction sequence as that shown in Scheme 1. Enantiomeric purity of amines (2*R*,6*S*)-(+)-**10a** and (2*S*,6*R*)-(–)-**10a**, determined by ¹H NMR spectroscopy in comparison with the spectrum of racemic compound **10a** and on addition of the chiral shift reagent (*R*)-(+)- α -methoxy- α -(trifluoromethyl)phenylacetic acid [(+)-MTPA],³¹ was found to be >98% (detection limit) for both enantiomers. In fact, the spectrum of racemic **10a** in the presence of (+)-MTPA showed a double doublet at δ 1.05 ppm for the 6-methyl protons, whereas only one doublet was observed for (2*R*,6*S*)-(+)-**10a** and (2*S*,6*R*)-(–)-**10a** at δ 1.02 and 1.06 ppm, respectively.

3. Results and discussion

The muscarinic activity of compounds **1–5** was evaluated by functional studies performed on classical preparations: rabbit stimulated vas deferens (M₁),³² guinea-pig stimulated left atria (M₂),³³ guinea-pig ileum (M₃),^{34,35} and guinea-pig lung strips (M₄).³⁶ Concerning this, it is appropriate to mention that the contraction of rabbit vas deferens was for a long time considered to be an ef-

fect mediated by M₁ receptor subtypes,³² even though more recent studies attribute the same effect to M₄-activation.³⁷ Therefore, since the pharmacological characterization of the receptor subtype involved does not appear to be clearly established, in the present work the rabbit vas deferens will be considered a putative M₁ subtype. The functional data of the new compounds, reported in Table 1, are expressed as pD₂ (–log ED₅₀, agonist potency), or as pK_b (antagonist potency) and as α (intrinsic activity). Carbachol was included in the study as reference compound and the two enantiomers of (\pm)-**2a** [(2*R*,5*R*)-(+)-**2a** and (2*S*,5*S*)-(–)-**2a**]³⁸ are reported for useful comparison. Moreover, the muscarinic activity of compounds (\pm)-**4a**, its two enantiomers (2*R*,6*S*)-(+)-**4a** and (2*S*,6*R*)-(–)-**4a**, (\pm)-**4b**, and carbachol was also evaluated by functional studies performed with a cytosensor microphysiometry instrument (Molecular Devices, Sunnyvale, CA, USA) on stably transfected CHO (Chinese hamster ovary) cells expressing the human M₁–M₅ receptors according to the procedure reported in the literature.³⁹ The concentration–effect curves were constructed as a peak acidification response, seen at increasing concentrations of the agonist, and pEC₅₀ values (–log EC₅₀) are reported in Table 2.

The analysis of data shows that all the compounds are full agonists at M₁–M₃ muscarinic receptor subtypes, except for compounds **3a** and (2*S*,6*R*)-(–)-**4a** at M₁ and compound **5b** at M₁ and M₂, which are not able to activate these subtypes and, when tested as antagonists, proved inactive up to 10 μ M. Concerning the M₄ subtype, the behavior of the tested compounds is various: in fact, most of them are full agonists, (\pm)-**4a** and (2*S*,6*R*)-(–)-**4a** have nearly full-intrinsic activity (α = 0.81 and 0.75, respectively), **3a** and **4b** behave as partial agonists, and **5a** and **5b** are weak antagonists. Analogously to carbachol, all the compounds display higher potency values toward M₂ and M₃ subtypes with respect to the others, except for compound **3a**, which is more active toward the M₄ subtype. Interestingly, the biological behaviors of the two higher homologues of **1a** (compounds **3a** and **4a**) are different. The enlargement of the 1,3-dioxolane nucleus of **1a** by inserting a methylene group between the 1-oxygen atom and the 4-side chain, affording **3a**, alters both activity and selectivity toward muscarinic receptors. In fact, compound **3a**, not activating M₁ subtype and being significantly more active than **1a** at M₄, and, above all, 155-fold and 91-fold less active at M₂ and M₃, respectively, proves to be selective for the M₄ subtype. Instead, compound **4a**, obtained by inserting a methylene group between the 1-oxygen atom and the 2-carbon atom of **1a**, shows pD₂ values not significantly different from those of **1a**, allowing the same interaction mechanism to be hypothesized. In the absence of experimental data regarding the accurate X-ray structure of any of the muscarinic receptor subtypes which might help to formulate a sound hypothesis on the receptor–ligand interaction pattern, a plausible way to interpret the biological profiles of different compounds is the use of the so-called active analogue approach; this ranks the biological profile of similar compounds also according to the comparison of some basic three-dimensional features of molecules (i.e.,



Scheme 2. Reagents: (a) $\text{ClCH}_2\text{COCH}_3$, TsOH, toluene; (b) $\text{Pd}(\text{OH})_2$, methanol; (c) powdered KOH; (d), LiAlH_4 , AlCl_3 , diethyl ether; (e) *p*-TsCl, pyridine; (f) $(\text{CH}_3)_2\text{NH}$, benzene; (g) CH_3I , diethyl ether.

molecular volume, interatomic distances, partial charges, dipole orientation, etc.) which can nowadays be easily calculated and visualized through molecular modeling tools.

In our case, the pharmacological data of compounds **3a** and **4a** might be analyzed by the overlapping of their low-energy conformations with that of the highly active compound **1a**. In fact, the molecular overlay of **1a** and **4a** shows that similar spatial regions are occupied by the presumed pharmacophore points, such as the basic methylated nitrogen atoms, the polar oxygen atoms, and the methyl substituents (Fig. 4a), whereas the introduction of a methylene group between the 1-oxygen atom and the 4-side chain of **1a**, affording **3a**, seems to produce a slight increase of the steric hindrance in the 1-oxygen atom interaction area (Fig. 4b).

This hypothesis might also be supported by inspection of the molecular interaction fields computed around the molecular surface of the two compounds; these fields highlight a more extended region around the 1-oxygen

atom of the 1,3-dioxolane ring in the case of **1a**; on the other hand, this cannot be equally observed for **3a**, probably due to the presence of an extra methylene group. The presence of more than one polar residue in the receptor site may be postulated; these residues might interact with the two properly oriented lone pairs of the 1-oxygen atom of **1a**, resulting in a stronger hydrogen bond (Fig. 4c). A steric clash should hamper such interaction with the receptor counterpart in the case of **3a**.

A similar interpretation might be given also in the case of the thio isoster of **4a** considered in this study. In fact, the replacement of the 4-oxygen atom of 1,4-dioxane compound **4a** with a sulfur atom, affording **5a**, significantly reduces the potency at all the muscarinic receptor subtypes, unlike what occurs by carrying out the same modification on the 1,3-dioxolane derivative **1a**, whose sulfur analogue **2a** shows a comparable pharmacological profile.

The different effects produced by the same modification carried out on compounds **1a** and **4a**, that is the replacement of the oxygen atom in position 1 and 4,

Table 1. Potency expressed as $-\log\text{ED}_{50}$ (pD_2), intrinsic activity (α)^a and dissociation constant ($\text{p}K_b$)^b of compounds **1–5** at M_1 – M_4 muscarinic receptor subtypes^c

Compound	Rabbit vas deferens (M_1)		Guinea-pig atrium (M_2)		Guinea-pig ileum (M_3)		Guinea-pig lung (M_4)	
	α	pD_2 ($\text{p}K_b$)	α	pD_2 ($\text{p}K_b$)	α	pD_2 ($\text{p}K_b$)	α	pD_2 ($\text{p}K_b$)
Carbachol	— ^d	—	1	7.33 ± 0.08	1	6.68 ± 0.01	1	5.43 ± 0.03
1a	—	—	1	7.43 ± 0.11	>1	7.69 ± 0.13	>1	5.80 ± 0.19
1b	—	—	1	6.73 ± 0.15	>1	7.47 ± 0.15	>1	5.71 ± 0.05
(\pm)- 2a	1	6.81 ± 0.09	1	7.40 ± 0.05	1	7.75 ± 0.02	1	6.15 ± 0.04
(2 <i>R</i> ,5 <i>R</i>)-(+)- 2a				7.54 ± 0.10^e		8.06 ± 0.04^e		
(2 <i>S</i> ,5 <i>S</i>)-(–)- 2a				5.37 ± 0.05^e		5.82 ± 0.06^e		
3a		(<5) ^f	1	5.24 ± 0.29	1	5.73 ± 0.15	0.54 ± 0.06	6.41 ± 0.04
(\pm)- 4a	1	5.65 ± 0.06	1	7.57 ± 0.11	1	7.34 ± 0.13	0.81 ± 0.07	5.90 ± 0.14
4b	1	5.08 ± 0.24	1	6.66 ± 0.19	1	6.02 ± 0.16	0.53 ± 0.07	6.01 ± 0.03
(2 <i>R</i> ,6 <i>S</i>)-(+)- 4a	1	6.78 ± 0.04	1	6.80 ± 0.10	1	7.65 ± 0.12	1	5.87 ± 0.15
(2 <i>S</i> ,6 <i>R</i>)-(–)- 4a		(<5) ^f	1	7.35 ± 0.21	1	6.53 ± 0.16	0.75 ± 0.11	4.34 ± 0.20
5a	1	4.46 ± 0.15	1	6.26 ± 0.16	1	6.46 ± 0.23		(5.14 ± 0.02)
5b		(<5) ^f		(<5) ^f	1	5.21 ± 0.10		(5.42 ± 0.05)

^a Intrinsic activity was measured by the ratio between the maximum response of the agonist and the maximum response of McN-A-343 at M_1 , and arecaidine propargyl ester (APE) at M_2 , M_3 , and M_4 subtypes.

^b Dissociation constants were calculated from the equation: $\log(\text{DR}-1) = \log[\text{ant}] - \log K_b$ according to van Rossum.⁴⁶

^c The results are means (\pm SEM) of four to six independent experiments.

^d Not determined.

^e Data from Ref. 38.

^f This compound showed no agonist activity and, when tested as antagonist, proved inactive up to 10 μM .

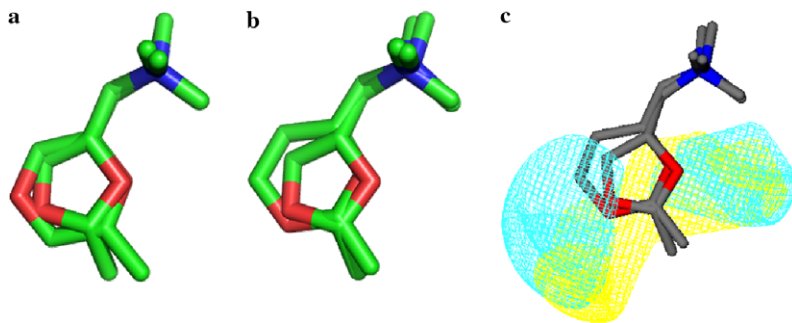
Table 2. Potency expressed as $-\log\text{EC}_{50}$ (pEC_{50})^a and intrinsic activity (α)^b of compounds (\pm)-**4a**, (\pm)-**4b**, (2*R*,6*S*)-(+)-**4a**, (2*S*,6*R*)-(–)-**4a**, and carbachol at human cloned M_1 – M_5 receptor subtypes

Compound	hM ₁		hM ₂		hM ₃		hM ₄		hM ₅	
	α	pEC_{50}								
Carbachol	1	4.30 ± 0.04	1	4.19 ± 0.06	1	5.74 ± 0.04	1	5.40 ± 0.03	1	4.96 ± 0.06
(\pm)- 4a	1	4.41 ± 0.05	1	4.31 ± 0.07	>1	6.56 ± 0.04	1	5.60 ± 0.07	1	5.10 ± 0.04
(\pm)- 4b	1	3.31 ± 0.03	1	3.11 ± 0.05	1	4.25 ± 0.05	1	3.55 ± 0.05	1	3.16 ± 0.03
(2 <i>R</i> ,6 <i>S</i>)-(+)- 4a	1	5.08 ± 0.06	1	4.43 ± 0.02	1	6.39 ± 0.05	1	5.55 ± 0.08	1	5.43 ± 0.04
(2 <i>S</i> ,6 <i>R</i>)-(–)- 4a	0.8	3.10 ± 0.05	1	4.81 ± 0.06	1	4.30 ± 0.07	1	4.60 ± 0.04	—	NA ^c

^a Determined by applying the cytosensor microphysiometry system to study the five human M_1 – M_5 muscarinic subtypes expressed in CHO cells.

^b Intrinsic activity was measured by the ratio between the maximum response of the agonist and the maximum response of carbachol.

^c NA, not active (intrinsic activity <0.3).

**Figure 4.** (a) Molecular overlays of compounds **1a** and **4a**; (b) **1a** and **3a**. (c) Molecular interaction fields for compounds **1a** (cyan) and **3a** (yellow) contoured at -3.0 kcal/mol.

respectively, with a sulfur one, might be explained by overlapping **1a** and **2a** (Fig. 5a) and **1a**, **4a**, and **5a** (Fig. 5b), a good overlay being obtained only in the case of **1a** and **2a**.

The analysis of data relative to the three pairs of isomers (**1a/1b**, **4a/4b**, **5a/5b**) shows that the stereochemical rela-

tionship between the side chain and the methyl group is not important either for the activation of M_4 subtype (pairs **1a/1b** and **4a/4b**) or for its blocking (pair **5a/5b**). Different behaviors may be observed when M_2 and M_3 subtypes are considered. In fact, while the two isomers **1a** and **1b** show similar agonist activities at the M_3 subtype and the *cis* isomer is only slightly more active than

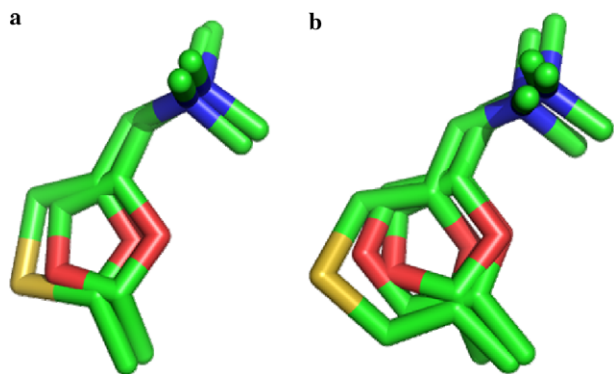


Figure 5. (a) Molecular overlays of compounds **1a** and **2a**; (b) **1a**, **4a**, and **5a**.

the *trans* isomer at the M_2 , in the case of the pairs **4a/4b** and **5a/5b**, the differences of activities are more evident, since the *cis* isomers are significantly more active than the corresponding *trans* isomers at both M_2 and M_3 subtypes. Therefore, for compounds bearing hexacyclic nuclei, the stereochemical relationship between the 2-side chain and the 6-methyl group plays an important role in drug–receptor interaction.

Moreover, none of the *cis* compounds is able to discriminate between the M_2 and M_3 subtypes. On the contrary, in the case of the *trans* compounds a slight but significant preferential activation of one of these two subtypes may be observed. Among them, the behavior of compound **5b**, which exclusively activates the ileal M_3 receptor subtype, though with a not very high pD_2 value, is extremely interesting. Such a marked M_3 -selectivity, which is particularly significant due to the complete lack of activity toward M_2 , makes this compound a useful tool for the characterization of the M_3 -mediated functions and for the design of new muscarinic receptor agonists selective for this subtype.

The comparison of the biological profiles of the two enantiomers of the most active compound (\pm)-**4a** among those bearing a hexacyclic nucleus is noteworthy. Also in this case, a significant selectivity for M_2 or M_3 muscarinic subtypes, absent in all the *cis* racemic isomers, may be observed for the two enantiomers (2*R*,6*S*)-(+)-**4a** and (2*S*,6*R*)-(–)-**4a**. In fact, (2*R*,6*S*)-(+)-**4a** is significantly more potent at M_3 with respect to M_1 , M_2 , and M_4 subtypes, whereas its optical antipode (2*S*,6*R*)-(–)-**4a** shows a different biological profile, since it is unable to activate M_1 subtype ($pK_b < 5$) and is more active at M_2 with respect to M_3 and M_4 (7- and 1023-fold, respectively). Moreover, (2*R*,6*S*)-(+)-**4a** is more potent than (2*S*,6*R*)-(–)-**4a** at M_3 and M_4 subtypes with eudismic ratios (ER) of 13 and 34, respectively, and, above all, behaves as a full agonist at M_1 subtype, which is not activated by (2*S*,6*R*)-(–)-**4a**. In the case of the M_2 subtype, the eutomer is the levorotatory form (2*S*,6*R*)-(–)-**4a** (ER = 4), an interesting reversal enantioselectivity being obtained. These data are quite interesting since, in the case of the oxathiolane agonist (\pm)-**2a**, the eutomer is the enantiomer (2*R*,5*R*)-(+)-**2a** for both M_2 and M_3 subtypes. Therefore, the selectivity of (2*S*,6*R*)-(–)-**4a** for M_2

with respect to the other muscarinic receptor subtypes is noteworthy due to the evidence that the configurations of its stereogenic centers are the opposite of those of the eutomer of (\pm)-**2a**. The above results are also confirmed by the data of compounds (\pm)-**4a**, its two enantiomers [(2*R*,6*S*)-(+)-**4a** and (2*S*,6*R*)-(–)-**4a**], and (\pm)-**4b** obtained on CHO cells (Table 2), though the pD_2 values are lower than those performed on tissues (Table 1). These differences may not represent an anomaly because in screening procedures a homogeneous population of cloned receptors is used, which can be organized differently to native receptors in functional tissues and, consequently, their biological behavior may not be coincident.

Therefore, clearly, all the muscarinic subtypes prove to have stereospecific requirements, whose characterization might be useful for the design of selective ligands.

In conclusion, this study suggests that hexacyclic 1,4-dioxane and 1,4-oxathiane compounds might represent suitable templates for the design of new muscarinic ligands and that, depending on ligand structure, a *cis* and *trans* relationship between the 2-side chain and the 6-methyl group might play an important role for a preferential muscarinic subtype activation.

4. Experimental

4.1. Chemistry

Melting points were taken in glass capillary tubes on a Büchi SMP-20 apparatus and are uncorrected. IR and ^1H NMR spectra were recorded on Perkin-Elmer 297 and Varian EM-390 instruments, respectively. Chemical shifts are reported in parts per million (ppm) relative to tetramethylsilane (TMS), and spin multiplicities are given as s (singlet), br s (broad singlet), d (doublet), t (triplet), q (quartet), or m (multiplet). Although the IR spectral data are not included because of the lack of unusual features, they were obtained for all compounds reported and were consistent with the assigned structures. The elemental compositions of the compounds were performed by the Microanalytical Laboratory of our department and agreed to within $\pm 0.4\%$ of the calculated value. When the elemental analysis was not included, crude compounds were used in the next step without further purification. Optical rotation was measured at a 1 g/100 mL concentration ($c = 1$), unless otherwise stated, with a Perkin-Elmer 241 polarimeter (accuracy $\pm 0.002^\circ$). Chromatographic separations were performed on silica gel columns (Kieselgel 40, 0.040–0.063 mm, Merck) by flash chromatography. Compounds were named following IUPAC rules as applied by Beilstein-Institut AutoNom (version 2.1), a software for systematic names in organic chemistry. Carbachol and compound **2a** were commercially available (RBI-Sigma).

4.1.1. *cis/trans*-(4*S*)-4-Benzoyloxymethyl-2-chloromethyl-2-methyl-[1,3]dioxolane [(4*S*)-12**].** A solution of chloroacetone (2.5 g, 27.0 mmol), (*R*)-3-benzyloxy-propane-1,2-diol (5.0 g, 27 mmol), and *p*-toluenesulfonic acid

(0.07 g, 0.44 mmol) in toluene (30 mL) was refluxed with vigorous stirring and in a Stark apparatus for 6 h. After cooling, the mixture was washed with Na₂CO₃ saturated solution (50 mL) and dried over Na₂SO₄. Evaporation of the solvent gave a residue, which was purified by column chromatography. Eluting with cyclohexane/EtOAc (9:1) afforded (4*S*)-**12** as a *cis/trans* mixture (ratio 1:1): 6.03 g (87% yield); ¹H NMR (CDCl₃) δ 1.44 and 1.51 (two s, 6, CH₃; *cis* and *trans*), 3.42–4.48 (m, 14, CH₂O, CH₂Cl and OCHCH₂; *cis* and *trans*), 4.60 (s, 4, CH₂Ar; *cis* and *trans*), 7.24–7.39 (m 10, ArH; *cis* and *trans*).

4.1.2. *cis/trans*-(4*R*)-4-Benzoyloxymethyl-2-chloromethyl-2-methyl-[1,3]dioxolane [(4*R*)-12**].** This was prepared as a *cis/trans* mixture (ratio 1:1) as described for (4*S*)-**12** starting from (*S*)-3-benzyloxy-propane-1,2-diol (5.0 g, 27.0 mmol): 6.0 g (87% yield). The ¹H NMR spectrum was identical to that of (4*S*)-**12**.

4.1.3. *cis/trans*-(4*S*)-(2-Chloromethyl-2-methyl-[1,3]dioxolan-4-yl)-methanol [(4*S*)-13**].** 20% Pd(OH)₂/C (0.4 g, 0.57 mmol) was added to a solution of (4*S*)-**12** (6.03 g, 23.5 mmol) in MeOH (40 mL) and the mixture was mechanically shaken under 50 psi of H₂ in a Parr apparatus for 3 h. The catalyst was removed by Millipore filtration, and the solvent was evaporated to give (4*S*)-**13** as a *cis/trans* mixture (ratio 1:1): 3.8 g (97% yield); ¹H NMR (CDCl₃) δ 1.46 and 1.52 (two s, 6, CH₃; *cis* and *trans*), 1.73 (br s, 2, OH; *cis* and *trans*), 3.47–4.42 (m, 14, CH₂O, CH₂Cl and OCHCH₂; *cis* and *trans*).

4.1.4. *cis/trans*-(4*R*)-(2-Chloromethyl-2-methyl-[1,3]dioxolan-4-yl)-methanol [(4*R*)-13**].** This was prepared as a *cis/trans* mixture (ratio 1:1) as described for (4*S*)-**13** starting from (4*R*)-**12** (6.0 g, 23.4 mmol): 3.5 g (90% yield). The ¹H NMR spectrum was identical to that of (4*S*)-**13**.

4.1.5. (1*S*,5*R*)-(–)-5-Methyl-3,6,8-trioxa-bicyclo[3.2.1]octane [(1*S*,5*R*)-(–)-14**].** A mixture of (4*S*)-**13** (3.8 g, 22.8 mmol) and powdered KOH (1.90 g, 33.9 mmol) was heated until an exothermic reaction developed. After cooling, the residue was distilled (61–62 °C/130 mm Hg): 2.9 g (98% yield); [α]_D²⁰ –31.41 (*c* 1, CHCl₃); ¹H NMR (CDCl₃) δ 1.38 (s, 3, CH₃), 3.52–4.83 (m, 7, trioxa-bicyclo).

4.1.6. (1*R*,5*S*)-(+)-5-Methyl-3,6,8-trioxa-bicyclo[3.2.1]octane [(1*R*,5*S*)-(+)-14**].** This was prepared as described for (1*S*,5*R*)-**14** starting from (4*R*)-**13** (3.5 g, 21.0 mmol): 2.5 g (92% yield); [α]_D²⁰ +30.95 (*c* 1, CHCl₃). The ¹H NMR spectrum was identical to that of (1*S*,5*R*)-**14**.

4.1.7. (2*R*,6*S*)-(+)- and (2*R*,6*R*)-(6-Methyl-[1,4]dioxan-2-yl)-methanol [(2*R*,6*S*)-(+)-6a** and (2*R*,6*R*)-**6b**].** A solution of AlCl₃ (3.0 g, 23.0 mmol) in diethyl ether (23 mL) was added dropwise over 3 min to a stirred solution of (1*S*,5*R*)-**14** (3.0 g, 23.0 mmol) and LiAlH₄ (0.9 g, 23.0 mmol) in diethyl ether (53 mL). The reaction mixture was refluxed vigorously until the starting material disappeared. Then it was cooled to 0 °C and quenched cautiously by the dropwise addition of Na₂SO₄ saturated solution. The solid was filtered off and the filtrate was

dried over Na₂SO₄. Removal of the solvent gave an oil, which was purified by column chromatography eluting with cyclohexane/EtOAc (7:3). The *cis* isomer (2*R*,6*S*)-**6a** eluted first: 0.8 g (26% yield); [α]_D²⁰ +13.40 (*c* 1, CH₃OH); ¹H NMR (CDCl₃) δ 0.99 (d, 3, CH₃), 2.95–3.64 (m, 8, cyclo and CH₂O), 4.62 (br s, 1, OH). The second fraction was the *trans* isomer (2*R*,6*R*)-**6b**: 0.08 g (3% yield); ¹H NMR (CDCl₃) δ 1.04 (d, 3, CH₃), 3.10–3.74 (m, 8, cyclo and CH₂O), 4.62 (br s, 1, OH).

4.1.8. (2*S*,6*R*)-(–)- and (2*S*,6*S*)-(6-Methyl-[1,4]dioxan-2-yl)-methanol [(2*S*,6*R*)-(–)-6a** and (2*S*,6*S*)-**6b**].** These were prepared as described for (2*R*,6*S*)-**6a** and (2*R*,6*R*)-**6b** starting from (1*R*,5*S*)-**14** (3.5 g, 27.0 mmol). The *cis* isomer (2*S*,6*R*)-**6a** eluted first: 0.8 g (23% yield); [α]_D²⁰ –13.29 (*c* 1, CH₃OH). The ¹H NMR spectrum was identical to that of (2*R*,6*S*)-**6a**. The second fraction was the *trans* isomer (2*S*,6*S*)-**6b**: 0.07 g (2% yield). The ¹H NMR spectrum was identical to that of (2*R*,6*R*)-**6b**.

4.1.9. Toluene-4-sulfonic acid (2*S*,6*S*)-(+)-6-methyl-[1,4]dioxan-2-ylmethyl ester [(2*S*,6*S*)-(+)-8a**].** Tosyl chloride (3.56 g, 18.7 mmol) was added to a stirred solution of (2*R*,6*S*)-**6a** (1.7 g, 12.9 mmol) in pyridine (20 mL) at 0 °C over 30 min. After being stirred for 3 h at 0 °C, the mixture was left for 20 h at 4 °C in the freezer. Then it was poured into ice and concentrated HCl (20 mL) and extracted with CHCl₃. The organic layers were washed with HCl 2 N (60 mL), NaHCO₃ saturated solution (60 mL), and H₂O (60 mL) and then dried over Na₂SO₄. The solvent was concentrated in vacuo to give a residue, which was purified by column chromatography. Eluting with cyclohexane/EtOAc (9:1) afforded (2*S*,6*S*)-**8a**: 2.0 g (54 % yield); [α]_D²⁰ +1.30 (*c* 1, CHCl₃); ¹H NMR (CDCl₃) δ 1.09 (d, 3, CH₃), 2.23 (s, 3, ArCH₃), 3.20–4.39 (m, 8, cyclo and CH₂O), 7.39 (d, 2, ArH), 7.81 (d, 2, ArH).

4.1.10. Toluene-4-sulfonic acid (2*R*,6*R*)-(–)-6-methyl-[1,4]dioxan-2-ylmethyl ester [(2*R*,6*R*)-(–)-8a**].** This was prepared as described for (2*S*,6*S*)-**8a** starting from (2*S*,6*R*)-**6a** (0.82 g, 6.2 mmol): 1.25 g (70% yield); [α]_D²⁰ –1.19 (*c* 1, CHCl₃). The ¹H NMR spectrum was identical to that of (2*S*,6*S*)-**8a**.

4.1.11. *cis*-Toluene-4-sulfonic acid 6-methyl-[1,4]dioxan-2-ylmethyl ester (8a**).** This was prepared as described for (2*S*,6*S*)-**8a** starting from **6a**²⁸ (1.1 g, 8.3 mmol): 1.92 g (81% yield). The ¹H NMR spectrum was identical to that of (2*S*,6*S*)-**8a**.

4.1.12. *trans*-Toluene-4-sulfonic acid 6-methyl-[1,4]dioxan-2-ylmethyl ester (8b**).** This was prepared as described for (2*S*,6*S*)-**8a** starting from **6b**²⁸ (0.55 g, 4.2 mmol): 0.96 g (81% yield); ¹H NMR (CDCl₃) δ 1.09 (d, 3, CH₃), 2.45 (s, 3, ArCH₃), 3.13–4.38 (m, 8, cyclo and CH₂O), 7.35 (d, 2, ArH), 7.80 (d, 2, ArH).

4.1.13. *cis*-Toluene-4-sulfonic acid 6-methyl-[1,4]oxathian-2-ylmethyl ester (9a**).** This was prepared as described for (2*S*,6*S*)-**8a** starting from **7a**²⁹ (1.9 g, 12.8 mmol): 3.55 g (91% yield); ¹H NMR (CDCl₃) δ 1.12 (d, 3,

CH₃), 2.17–2.53 (m, 4, CH₂SCH₂), 2.41 (s, 3, ArCH₃), 3.55–4.02 (m, 4, CHOCHCH₂O), 7.31 (d, 2, ArH), 7.77 (d, 2, ArH).

4.1.14. *trans*-Toluene-4-sulfonic acid 6-methyl-[1,4]oxathian-2-ylmethyl ester (9b). This was prepared as described for (2*S*,6*S*)-**8a** starting from **7b**²⁹ (1.4 g, 9.5 mmol): 1.6 g (56% yield); ¹H NMR (CDCl₃) δ 1.22 (d, 3, CH₃), 2.28–2.78 (m, 4, CH₂SCH₂), 2.46 (s, 3, ArCH₃), 3.82–4.37 (m, 4, CHOCHCH₂O), 7.35 (d, 2, ArH), 7.80 (d, 2, ArH).

4.1.15. (2*R*,6*S*)-(+)-Dimethyl-(6-methyl-[1,4]dioxan-2-ylmethyl)-amine [(2*R*,6*S*)-(+)-10a**].** A solution of (2*S*,6*S*)-**8a** (0.7 g, 2.4 mmol) and dimethylamine (5.5 mL) in dry benzene (10 mL) was heated in a sealed tube for 60 h at 120 °C. After evaporation of the solvent, the residue was dissolved in CHCl₃, which was washed with NaOH 2 N and dried over Na₂SO₄. The solvent was concentrated in vacuo to give a residue, which was purified by column chromatography. Eluting with CHCl₃/CH₃OH (9:1) afforded (2*R*,6*S*)-**10a** as the free base: 0.3 g (77% yield); [α]_D²⁰ +12.24 (*c* 1, CHCl₃); ¹H NMR (CDCl₃) δ 1.10 (d, 3, CH₃), 2.12–2.43 (m, 2, CH₂N), 2.26 (s, 6, N(CH₃)₂), 3.08–3.24 (m, 2, cyclo), 3.56–3.81 (m, 4, cyclo); enantiomeric purity was >98% (detection limit), determined with (+)-MTPA³¹ as the chiral shift reagent.

4.1.16. (2*S*,6*R*)-(–)-Dimethyl-(6-methyl-[1,4]dioxan-2-ylmethyl)-amine [(2*S*,6*R*)-(–)-10a**].** This was prepared as described for (2*R*,6*S*)-**10a** starting from (2*R*,6*R*)-**8a** (0.8 g, 2.8 mmol): 0.4 g (89% yield); [α]_D²⁰ –12.49 (*c* 1, CHCl₃). The ¹H NMR spectrum was identical to that of (2*R*,6*S*)-**10a**. Enantiomeric purity was >98% (detection limit), determined with (+)-MTPA³¹ as the chiral shift reagent.

4.1.17. *cis*-Dimethyl-(6-methyl-[1,4]dioxan-2-ylmethyl)-amine (10a). This was prepared as described for (2*R*,6*S*)-**10a** starting from **8a** (1.92 g, 6.7 mmol): 0.74 g (69% yield). The ¹H NMR spectrum was identical to that of (2*R*,6*S*)-**10a**.

4.1.18. *trans*-Dimethyl-(6-methyl-[1,4]dioxan-2-ylmethyl)-amine (10b). This was prepared as described for (2*R*,6*S*)-**10a** starting from **8b** (0.5 g, 1.7 mmol): 0.2 g (71% yield); ¹H NMR (CDCl₃) δ 1.20 (d, 3, CH₃), 2.30 (s, 6, N(CH₃)₂), 2.35–2.62 (m, 2, CH₂N), 3.30–3.52 (m, 2, cycle), 3.68–3.73 (m, 2, cyclo), 3.83–4.11 (m, 2, cyclo).

4.1.19. *cis*-Dimethyl-(6-methyl-[1,4]oxathian-2-ylmethyl)-amine (11a). This was prepared as described for (2*R*,6*S*)-**10a** starting from **9a** (1.4 g, 4.6 mmol): 0.6 g (74% yield); ¹H NMR (CDCl₃) δ 1.20 (d, 3, CH₃), 2.23 (s, 6, N(CH₃)₂), 2.26 (m, 6, CH₂SCH₂ and CH₂N), 3.75 (m, 2, CHOCH).

4.1.20. *trans*-Dimethyl-(6-methyl-[1,4]oxathian-2-ylmethyl)-amine (11b). This was prepared as described for (2*R*,6*S*)-**10a** starting from **9b** (1.4 g, 4.6 mmol): 0.4 g (49% yield); ¹H NMR (CDCl₃) δ 1.36 (d, 3, CH₃),

2.22 (s, 6, N(CH₃)₂), 2.30–2.80 (m, 6, CH₂SCH₂ and CH₂N), 4.02 (m, 1, CHO), 4.10 (m, 1, CHO).

4.1.21. (2*R*,6*S*)-(+)-Trimethyl-(6-methyl-[1,4]dioxan-2-ylmethyl)-ammonium iodide [(2*R*,6*S*)-(+)-4a**].** A solution of (2*R*,6*S*)-**10a** (0.4 g, 2.5 mmol) in diethyl ether (15 mL) was treated with an excess of methyl iodide and left at rt in the dark for 24 h. The solid was filtered and recrystallized from 2-PrOH; mp 200 °C; [α]_D²⁰ +38.91 (*c* 1, CH₃OH); ¹H NMR (DMSO) δ 1.07 (d, 3, CH₃), 2.99–3.10 (m, 2, CH₂N), 3.12 (s, 9, N(CH₃)₃), 3.45 (m, 2, cyclo), 3.60 (m, 2, cyclo), 3.80 (m, 1, cyclo), 4.21 (m, 1, cyclo). Anal. Calcd for C₉H₂₀INO₂: C, 35.89; H, 6.69; N, 4.65. Found: C, 35.91; H, 6.81; N, 4.55.

4.1.22. (2*S*,6*R*)-(–)-Trimethyl-(6-methyl-[1,4]dioxan-2-ylmethyl)-ammonium iodide [(2*S*,6*R*)-(–)-4a**].** This was prepared as described for (2*R*,6*S*)-**4a** starting from (2*S*,6*R*)-**10a** (0.5 g, 3.1 mmol): the solid was recrystallized from 2-PrOH; mp 200 °C; [α]_D²⁰ –39.01 (*c* 1, CH₃OH). The ¹H NMR spectrum was identical to that of (2*R*,6*S*)-**4a**. Anal. Calcd for C₉H₂₀INO₂: C, 35.89; H, 6.69; N, 4.65. Found: C, 35.78; H, 6.55; N, 4.39.

4.1.23. *cis*-Trimethyl-(6-methyl-[1,4]dioxan-2-ylmethyl)-ammonium iodide (4a). This was prepared as described for (2*R*,6*S*)-**4a** starting from **10a** (0.5 g, 3.1 mmol): the solid was recrystallized from 2-PrOH; mp 200 °C. The ¹H NMR spectrum was identical to that of (2*R*,6*S*)-**4a**. Anal. Calcd for C₉H₂₀INO₂: C, 35.89; H, 6.69; N, 4.65. Found: C, 35.77; H, 6.88; N, 4.45.

4.1.24. *trans*-Trimethyl-(6-methyl-[1,4]dioxan-2-ylmethyl)-ammonium iodide (4b). This was prepared as described for (2*R*,6*S*)-**4a** starting from **10b** (0.2 g, 1.3 mmol): the solid was recrystallized from 2-PrOH; mp 216–217 °C; ¹H NMR (DMSO) δ 1.10 (d, 3, CH₃), 3.12 (s, 9, N(CH₃)₃), 3.19–3.30 (m, 2, CH₂N), 3.50 (m, 2, cyclo), 3.62 (m, 2, cyclo), 4.00 (m, 2, cyclo). Anal. Calcd for C₉H₂₀INO₂: C, 35.89; H, 6.69; N, 4.65. Found: C, 35.81; H, 6.56; N, 4.48.

4.1.25. *cis*-Trimethyl-(6-methyl-[1,4]oxathian-2-ylmethyl)-ammonium iodide (5a). This was prepared as described for (2*R*,6*S*)-**4a** starting from **11a** (1.0 g, 5.7 mmol): the solid was recrystallized from EtOH; mp 193–194 °C; ¹H NMR (DMSO) δ 1.15 (d, 3, CH₃), 2.29–2.50 (m, 4, CH₂SCH₂), 3.10 (s, 9, N(CH₃)₃), 3.45 (m, 2, CH₂N), 3.89 (m, 1, CHO), 4.22 (m, 1, CHO). Anal. Calcd for C₉H₂₀INOS: C, 34.07; H, 6.35; N, 4.42; S, 10.11. Found: C, 34.25; H, 6.21; N, 4.18; S, 10.23.

4.1.26. *trans*-Trimethyl-(6-methyl-[1,4]oxathian-2-ylmethyl)-ammonium iodide (5b). This was prepared as described for (2*R*,6*S*)-**4a** starting from **11b** (1.4 g, 8.0 mmol): the solid was recrystallized from EtOH; mp 207–208 °C; ¹H NMR (DMSO) δ 1.20 (d, 3, CH₃), 2.40–2.80 (m, 4, CH₂SCH₂), 3.15 (s, 9, N(CH₃)₃), 3.35 (m, 2, CH₂N), 4.18 (m, 1, CHO), 4.55 (m, 1, CHO). Anal. Calcd for C₉H₂₀INOS: C, 34.07; H, 6.35; N, 4.42; S, 10.11. Found: C, 33.97; H, 6.38; N, 4.39; S, 10.35.

4.2. Molecular modeling

Molecular superpositions of compounds **1a**, **2a**, **3a**, **4a**, and **5a** were performed by means of the QXP software⁴⁰ as follows: initially molecular structures were built using standard bond length and valence angles; then reference compound **1a** was submitted to a 5000-steps Monte-Carlo conformational analysis run in order to assess the proper spatial arrangement with respect to the 1,3-dioxolane ring. Each of the other compounds was fitted onto the low energy conformation of the selected template according to the template fitting search algorithm implemented within the same QXP package. This procedure searches for the best superposition on the basis of attractive forces between similar atoms or functional groups in agreement with energetically permitted three-dimensional states.

During the conformational search, the geometry of the reference compound **1a** was kept fixed while the internal geometry of **3a** and **4a** was randomly perturbed for 5000 Monte-Carlo runs.

The GRID fields⁴¹ on the overlay showing the best superposition according to the QXP scoring function were in turn calculated, placing hydroxyl oxygen as atom probe on the nodes of a $86 \times 76 \times 76$ 0.2-Å-spaced cubic grid.

Images were rendered with the software PYMOL 0.99 (<http://pymol.sourceforge.net>).

4.3. X-ray crystal structure analysis of 10a picrate salt

Crystals of **10a** picrate salt were obtained by slow evaporation from H₂O/CH₃OH (3:1) solution. The X-ray data collection was performed at room temperature with an Oxford Diffraction Xcalibur PX Ultra CCD diffractometer, equipped with Onyx optics, using Cu-K α radiation ($\lambda = 1.5418$ Å). Intensity data were corrected for absorption by a multi-scan procedure.⁴² Crystal data: formula (C₈H₁₈NO₂)⁺(C₆H₂N₃O₇)⁻, $M_w = 388.34$, Monoclinic, Space group $P2_1/n$; $a = 6.9911(6)$ Å, $b = 10.4852(7)$ Å, $c = 25.039(2)$ Å, $\beta = 90.048(6)^\circ$, $V = 1835.4(2)$ Å³, $Z = 4$, $\mu = 1.024$ mm⁻¹. 14,527 reflections measured, 2530 unique ($R_{int} = 0.0322$), 2046 reflections with $I > 2\sigma_I$. $R[F^2 > 2\sigma(F^2)] = 0.0429$, $wR(F^2) = 0.1268$, $GoF = 1.047$, $\delta\rho_{max} = 0.252$, $\delta\rho_{min} = -0.136$ e Å⁻³. The structure was solved by direct methods, with SIR-97,⁴³ and refined by full-matrix least-squares with SHELXL-97,⁴⁴ applying a correction for twinning by merohedry (monoclinic pseudo-orthorhombic lattice; 0.60 major component). In the final refinement cycles (249 parameters, no restraints) all non-hydrogen atoms were refined anisotropically and hydrogens were in geometrically calculated positions, riding on the respective carrier atoms, each with an isotropic temperature factor linked to that of its carrier atom. For graphics ORTEP-3 was employed.⁴⁵

CCDC-619120 contains the supplementary crystallographic data for this paper. These data can be obtained free of charge at www.ccdc.cam.ac.uk/conts/retrieving.html or from the Cambridge Crystallographic Data

Centre, 12 Union Road, Cambridge CB2 1EZ, UK; fax: +44-1223-336033; e-mail: deposit@ccdc.cam.ac.uk.

4.4. Pharmacology

General considerations. Male guinea pigs (200–300 g) and male New Zealand white rabbits (3.0–3.5 kg) were killed by cervical dislocation. The organs required were set up rapidly under 1 g of tension in 20-mL organ baths containing physiological salt solution (PSS) maintained at an appropriate temperature and aerated with 5% CO₂–95% O₂. Dose–response curves were constructed by cumulative addition of the reference agonist. The concentration of agonist in the organ bath was increased approximately 3-fold at each step, with each addition being made only after the response to the previous addition had attained a maximal level and remained steady. After 30 min of washing, a cumulative dose–response curve to the agonist under study was constructed. When the compound in question behaved as an antagonist, following 30 min of washing, tissues were incubated with the antagonist for 30 min, and a new dose–response curve to the agonist was obtained. Responses were expressed as a percentage of the maximal response obtained in the control curve. Contractions were recorded by means of a force displacement transducer connected to the MacLab system PowerLab/800. In addition, parallel experiments, in which tissues did not receive any antagonist, were run in order to check any variation in sensitivity.

In all cases, parallel experiments in which tissues received only the reference agonist were run in order to check any variation in sensitivity.

All animal testing was carried out according to the European Community Council Directive of 24 November 1986 (86/609/EEC).

4.4.1. Rabbit stimulated vas deferens. This preparation was set up according to the method of Eltze.³² Vasa deferentia were carefully dissected free of surrounding tissue and were divided into four segments, two prostatic portions of 1 cm and two epididymal portions of approximately 1.5 cm length. The four segments were mounted in PSS with the following composition (mM): NaCl (118.4), KCl (4.7), CaCl₂ (2.52), MgCl₂ (0.6), KH₂PO₄ (1.18), NaHCO₃ (25.0), and glucose (11.1); 10⁻⁶ M yohimbine and 10⁻⁸ M tripitramine were included to block α_2 -adrenoceptors and M₂ muscarinic receptors, respectively. The solution was maintained at 30 °C, and tissues were stimulated through platinum electrodes by square-wave pulses (0.1 ms, 2 Hz, 10–15 V). Contractions were measured isometrically after tissues had been equilibrated for 1 h, and then a cumulative dose–response curve to *p*-Cl-McN-A-343 was constructed.

4.4.2. Guinea-pig ileum. Two-centimeter-long portions of terminal ileum were taken at about 5 cm from the ileum–cecum junction and mounted in PSS, at 37 °C, of the following composition (mM): NaCl (118.0), NaHCO₃ (23.8), KCl (4.7), MgSO₄–7H₂O (1.18), KH₂PO₄ (1.18), CaCl₂ (2.52), and glucose (11.7). Tension changes

were recorded isotonicity. Tissues were equilibrated for 30 min, and dose–response curves to arecaidine propargyl ester were obtained at 30-min intervals, the first one being discarded and the second being taken as control.

4.4.3. Guinea-pig stimulated left atrium. The heart was rapidly removed, and the right and left atria were separately excised. Left atria were mounted in PSS (the same as was used for ileum) at 30 °C and stimulated through platinum electrodes by square-wave pulses (1 ms, 1 Hz, 5–10 V) (Tetra Stimulus, N. Zagnoni). Inotropic activity was recorded isometrically. Tissues were equilibrated for 2 h and a cumulative dose–response curve to arecaidine propargyl ester was constructed.

4.4.4. Guinea-pig lung strips. The lungs were rapidly removed and strips of peripheral lung tissue were cut either from the body of a lower lobe with the longitudinal axis of the strip parallel to the bronchus or from the peripheral margin of the lobe. The preparations were mounted, with a preload of 0.3 g, in PSS with the following composition (mM): NaCl (118.78), KCl (4.32), CaCl₂·2H₂O (2.52), MgSO₄·7H₂O (1.18), KH₂PO₄ (1.28), NaHCO₃ (25.0), and glucose (5.55). Contractions were recorded isotonicity at 37 °C after tissues had been equilibrated for 1 h; then two cumulative dose–response curves to arecaidine propargyl ester (0.01, 0.1, 1, 10, and 100 mM) were obtained at 45-min intervals, the first one being discarded and the second being taken as control.

4.4.5. Measurement of extracellular acidification rates. CHO cells, stably expressing human mAChRs M₁–M₅, were supplied by Professor Tom I. Bonner (National Institute of Mental Health, Bethesda, MD, USA). Cells were maintained in α -minimum essential medium containing 10% fetal bovine serum at 37 °C under 5% CO₂–95% O₂; they were grown to confluence and harvested by scraping in fresh medium. Changes in extracellular acidification were determined using an eight-channel cytosensor microphysiometry instrument (Molecular Devices). Cells were seeded into cytosensor cell capsules 20 h prior to experiments at a density of 3 × 10⁵ cells per well. The cell capsules, mounted in sensor chambers, were placed on the instrument, and the cells were perfused with media via a peristaltic pump, during which the pH of the microenvironment surrounding the sensor was kept constant. The removal of acid from the cells by the perfusate was periodically halted (pump turned off), allowing a build up of acid metabolites and, therefore, a change in chamber pH (acidification rate). This on–off cycle was repeated throughout the experiment and the effect of compounds was determined by adding the compound to the chamber. The extracellular acidification rates were measured in each 120-s pump cycle; flow on at 100 μ l min⁻¹ for 90 s with a 20-s exposure to the test compound, flow off for 30 s. The acidification rate was determined between 98 and 118 s, using the cytosoft program (Molecular Devices). Concentration–effect curves were obtained by exposing the cells sequentially to increasing concentrations of agonist at intervals of 21 min.

4.4.6. Statistical analysis. The results are expressed as means \pm SEM Student's *t* test was used to assess the statistical significance of the difference between means.

Potency was expressed as $-\log$ ED₅₀ \pm SEM derived from dose–response curves and represents $-\log$ of the concentration of agonists to produce 50% of the maximum contraction.

Acknowledgments

The authors thank Dr. Francesca Ghelfi for her technical support in assays performed with the cytosensor microphysiometry instrument. This work was supported by grants from the MIUR (Rome) and the University of Camerino.

References and notes

- Eglen, R. M.; Choppin, A.; Watson, N. *Trends Pharmacol. Sci.* **2001**, *22*, 409.
- Lefkowitz, R. J. *Trends Pharmacol. Sci.* **2004**, *25*, 413.
- Wess, J.; Duttaroy, A.; Zhang, W.; Gomeza, J.; Cui, Y.; Miyakawa, T.; Bymaster, F. P.; McKinzie, L.; Felder, C. C.; Lamping, K. G.; Faraci, F. M.; Deng, C.; Yamada, M. *Receptor Channel* **2003**, *9*, 279.
- Caulfield, M. P.; Birdsall, N. J. M. *Pharmacol. Rev.* **1998**, *50*, 279.
- Ma, W.; Li, B.-S.; Zhang, L.; Pant, H. C. *Drug News Perspect.* **2004**, *17*, 258.
- Ashkenazi, A.; Ramachandran, J.; Capon, D. J. *Nature* **1989**, *340*, 146.
- Pedretti, A.; Vistoli, G.; Marconi, C.; Testa, B. *Chem. Biodiv.* **2006**, *3*, 481.
- Shi, L.; Javitch, J. A. *Annu. Rev. Pharmacol. Toxicol.* **2002**, *42*, 437.
- Fisher, A. *Expert Opin. Invest. Drugs* **1997**, *6*, 1395.
- DeLapp, N.; Wu, S.; Belagaje, R.; Johnstone, E.; Little, S.; Shannon, H.; Bymaster, F.; Calligaro, D.; Mitch, C.; Whitesitt, C.; Ward, J.; Sheardown, M.; Fink-Jensen, A.; Jeppesen, L.; Thomsen, C.; Sauerberg, P. *Biochem. Biophys. Res. Commun.* **1998**, *244*, 156.
- Felder, C. C.; Porter, A. C.; Skillman, T. L.; Zhang, L.; Bymaster, F. P.; Nathanson, N. M.; Hamilton, S. E.; Gomeza, J.; Wess, J.; McKinzie, D. L. *Life Sci.* **2001**, *68*, 2605.
- Duttaroy, A.; Gomeza, J.; Gan, J.-W.; Siddiqui, N.; Basile, A. S.; Harman, W. D.; Smith, P. L.; Felder, C. C.; Levey, A. I.; Wess, J. *Mol. Pharmacol.* **2002**, *62*, 1084.
- Wess, J.; Duttaroy, A.; Gomeza, J.; Zhang, W.; Yamada, M.; Felder, C. C.; Bernardini, N.; Reeh, P. W. *Life Sci.* **2003**, *72*, 2047.
- De Sarno, P.; Shestopal, S. A.; Zmijewska, A. A.; Jope, R. S. *Brain Res.* **2005**, *1041*, 112.
- Budd, D. C.; Spragg, E. J.; Ridd, K.; Tobin, A. B. *Biochem. J.* **2004**, *381*, 43.
- Angeli, P. *Il Farmaco* **1995**, *50*, 565.
- Triggle, D. J.; Belleau, B. *Can. J. Chem.* **1962**, *40*, 1201.
- Pigini, M.; Brasili, L.; Giannella, M.; Gualtieri, F. *Eur. J. Med. Chem.* **1981**, *16*, 415.
- Grana, E.; Lucchelli, A.; Zonta, F.; Santagostino-Barbone, M. G.; D'Agostino, G. *Naunyn Schmiedeberg's Arch. Pharmacol.* **1986**, *332*, 213.

20. Piergentili, A.; Angeli, P.; Gagliardi, R.; Gentili, F.; Giannella, M.; Marucci, G.; Pigini, M.; Quaglia, W. *Med. Chem. Res.* **2002**, *11*, 12.
21. Werner, L. H. U.S. Patent 2,903,464, 1959; *Chem. Abstr.* **1960**, *54*, 11544.
22. Smirnov, V. V.; Antonova, N. G.; Zotov, S. B.; Kvasnyuk-Mudryi, F. V.; Sitanova, N. A. *Khim. Geterotsykl. Soedin.* **1970**, *131*, 318; *Chem. Abstr.* **1970**, *73*, 66518.
23. Van Cauwenberghe, R.; Anteunis, M.; Valckx, L. *Bull. Soc. Chim. Belg.* **1974**, *83*, 285.
24. Anteunis, M. J. O.; Van Cauwenberghe, R.; Valckx, L.; Van Bever, W. F. M.; Van Nueten, J. M. *Eur. J. Med. Chem.* **1975**, *10*, 360.
25. Inch, T. D.; Williams, N. J. *Chem. Soc. (C)* **1970**, *2*, 263.
26. Ing, H. R. *Science* **1949**, *109*, 264.
27. Barlow, R. B. In *Introduction to Chemical Pharmacology*; Barlow, R. B., Ed.; Methuen, Wiley: London, New York, 1964; p 203.
28. Gelas, J.; Veysières-Rambaud, S. *Carbohydr. Res.* **1974**, *37*, 293.
29. Gelas, J.; Veysières-Rambaud, S. *Carbohydr. Res.* **1974**, *37*, 303.
30. Duclos, R. I., Jr.; Makriyannis, A. *J. Org. Chem.* **1992**, *57*, 6156.
31. Villani, F. J., Jr.; Costanzo, M. J.; Inners, R. R.; Mutter, M. S.; McClure, D. E. *J. Org. Chem.* **1986**, *51*, 3715.
32. Eltze, M. *Eur. J. Pharmacol.* **1988**, *151*, 205.
33. Kenakin, T. P.; Boselli, C. *Naunyn Schmiedeberg's Arch. Pharmacol.* **1991**, *344*, 201.
34. Ringdahl, B. *Mol. Pharmacol.* **1987**, *31*, 351.
35. Eglén, R. M.; Harris, G. C. *Br. J. Pharmacol.* **1993**, *109*, 946.
36. Roffel, A. F.; Elzinga, C. R. S.; Zaagsma, J. *Eur. J. Pharmacol.* **1993**, *250*, 267.
37. Budriesi, R.; Cacciaguerra, S.; Di Toro, R.; Bolognesi, M. L.; Chiarini, A.; Minarini, A.; Rosini, M.; Spampinato, S.; Tumiatti, V.; Melchiorre, C. *Br. J. Pharmacol.* **2001**, *132*, 1009.
38. Angeli, P.; Brasili, L.; Giannella, M.; Gualtieri, F.; Picchio, M. T.; Teodori, E. *Naunyn Schmiedeberg's Arch. Pharmacol.* **1988**, *337*, 241.
39. Wood, M. D.; Murkitt, K. L.; Ho, M.; Watson, J. M.; Brown, F.; Hunter, A. J.; Middlemiss, D. N. *Br. J. Pharmacol.* **1999**, *126*, 1620.
40. McMartin, C.; Bohacek, R. S. *J. Comput. Aided Mol. Des.* **1997**, *11*, 333.
41. Goodford, P. J. *J. Med. Chem.* **1985**, *28*, 849.
42. Oxford Diffraction, **2006**, *CrysAlisPro* (Version 1.171.29.2). Oxford Diffraction Ltd, Abingdon, Oxfordshire, England.
43. Altomare, A.; Burla, M. C.; Camalli, M.; Cascarano, G. L.; Giacovazzo, C.; Guagliardi, A.; Moliterni, A. G. G.; Polidori, G.; Spagna, R. *J. Appl. Crystallogr.* **1999**, *32*, 115.
44. Sheldrick, G. M. *SHELXL97, Program for Crystal Structure Refinement*; University of Göttingen, Göttingen: Germany, 1986.
45. Farrugia, L. J. *J. Appl. Crystallogr.* **1999**, *32*, 837.
46. van Rossum, J. M. *Arch. Int. Pharmacodyn. Ther.* **1963**, *143*, 299.